Theory of Deep Minima in $(e, 2e)$ Measurements of Triply Differential Cross Sections

J. H. Macek
Department of Physics and Astronomy, University of Tennessee, Knoxville, Tennessee 37496, USA and Physics Division, Oak Ridge National Laboratory, Oak Ridge, Tennessee 37831, USA

J. B. Sternberg and S. Y. Ovchinnikov*
Department of Physics and Astronomy, University of Tennessee, Knoxville, Tennessee 37496, USA

J. S. Briggs
Fakultät für Physik, Albert-Ludwigs-Universität, D-79104 Freiburg im Breisgau, Germany
(Received 24 August 2009; published 20 January 2010)

Deep minima in $He(e, 2e)He^+$ triply differential cross sections are traced to vortices in atomic wave functions. Such vortices have been predicted earlier, but the present calculations show that they have also been observed experimentally, although not recognized as vortices. Their observation in $(e, 2e)$ measurements shows that vortices play an important role in electron correlations related to the transfer of angular momentum between incident and ejected electrons. The vortices significantly extend the list of known features that summarize the general picture of electron correlations in impact ionization.

DOI: 10.1103/PhysRevLett.104.033201 PACS numbers: 34.50.Fa, 34.80.Pa

Measurements of the momentum distributions in electron scattering processes have long been used to study electron correlations in the two-electron final states [1]. Experiments where two outgoing electrons are measured in coincidence, namely $(e, 2e)$ measurements of triply differential cross sections (TDCS), have been of particular interest since they directly probe electron correlations in the final state. Because electron correlations are central to electron motion in atoms, molecules, and solids, a complete understanding of their effect in the most direct experimental observation of them, namely $(e, 2e)$ measurements, are of continuing interest for the quantum structure of any species containing two or more electrons. Theory is now able to accurately model $(e, 2e)$ processes for H-atom [2–4] and He-atom targets [5–8]. From these studies a general picture of $(e, 2e)$ electron correlations has emerged. This picture identifies structures in the $(e, 2e)$ electron distributions with a small number of specific interactions and quantum effects in two-electron wave functions [7,9]. It was speculated that the classifications given in Ref. [9] account for all structures that are observed, and that no further features would emerge in more accurate calculations and future experiments. In this Letter we show that the list in Ref. [9] is incomplete and that an unexplained feature [8] points to a new explanation for a pronounced minima observed in $(e, 2e)$ experiments [10–12].

The effects listed in Ref. [9] are quite comprehensive, but are unable to identify the origins of an isolated exact zero in the $(e, 2e)$ cross section. The exact zero is reproduced with theories employing highly correlated final states, but these calculations do not give a deeper understanding of how both the real and imaginary parts of transition matrix elements could vanish exactly at a point [8] rather than along a nodal surface. At best they can point to an "interference effect" as the origin of an exact zero in measured and calculated TDCS. In this Letter we will show that the exact zero in the theory of Ref. [8] and, by implication, in the measurements of Refs. [11,13], corresponds to a vortex in a correlated two-electron wave function. It is further shown that isolated zeros of transition matrix elements always correspond to vortices. This unexpected relevance of vortex motion to electron correlations in atoms and molecules provides a new tool to understand the dynamics of quantum systems. It also realizes an insight put forward earlier [14], namely, that vortices in atomic wave functions must have experimental consequences. The confirmation that vortex structures have been observed thereby opens the way for experimental study of this aspect of correlated electrons.

That vortices in atomic wave functions appear as observable zeros of electron momentum distributions emerges from time-dependent calculations of ionization by proton impact [15]. In those studies, vortices in the semiclassical, time-dependent wave functions form at times close to the time of impact and remain at large times corresponding to asymptotic distances $\boldsymbol{r} = \boldsymbol{k}t$ where electrons with momentum $\boldsymbol{k}$ are detected.

The relation between wave functions and momentum distributions is central to understanding vortices in momentum distributions. This relation has been called [15,16] the "imaging theorem." For one-electron species the relation is

$$\lim_{t\to\infty} t^{3/2}|\psi(\boldsymbol{r} = \boldsymbol{k}t, t)| = |A(\boldsymbol{k})|, \tag{1}$$

where $A(\boldsymbol{k})$ is the ionization amplitude in atomic units. This expression omits phase factors in the relation between wave functions and amplitudes. They are not important for vortex analysis since zeros are not affected by phases.

Equation (1) is often implicitly assumed in measurements of momentum distributions, yet the implications of the connection between ionization amplitudes and Schrödinger wave functions is seldom exploited to interpret structure in $A(\boldsymbol{k})$. This is understandable, since Eq. (1) is seldom used for actual calculations. It is implicit, however, that Eq. (1) may be helpful for interpreting structure even though it is not actually used to compute $A(\boldsymbol{k})$. That is the case here in that ionization amplitudes have properties of single-particle wave functions and zeros in these amplitudes can be analyzed using the theory of vortex dynamics given in Ref. [14]. Using that theory it is easy to show that a first order zero in the single-particle amplitude must be a vortex. Integration of the normalized probability current, called the velocity field $\boldsymbol{v} = \mathrm{Im}(\frac{\nabla\psi}{\psi})$ around a closed loop encircling the vortex equals 2π. Note also that this relation is not affected by analytic phase factors. By first order zero in an amplitude $A(\boldsymbol{k})$ we mean that the amplitude may be expanded in a power series about the zero $\boldsymbol{a}$, and the lowest order term is linear in $\boldsymbol{k} - \boldsymbol{a}$. This excludes zeros that appear owing to essential singularities as occurs, for example, due to the electron-electron interaction discussed in Ref. [8]. The vortex is characterized by a vortex line defined as a line along which both the real and imaginary parts of $A(\boldsymbol{k})$ vanish. All of these properties were verified for the zeros reported in Ref. [8].

To employ the imaging theorem for electron impact, a representation where the incident electron is described by a localized wave packet is used. Then both the incident electron a and the target electron b are initially localized in space. The final state is then an outgoing two-electron wave packet and one may set both $\boldsymbol{r}_a = \boldsymbol{k}_a t$ and $\boldsymbol{r}_b = \boldsymbol{k}_b t$ then take the limit as $t \to \infty$. In this case we have

$$\lim_{t\to\infty} t^3 |\psi(\boldsymbol{r_a} = \boldsymbol{k}_a t, \boldsymbol{r}_b = \boldsymbol{k}_b t, t)| = |A(\boldsymbol{k}_a, \boldsymbol{k}_b)| \quad (2)$$

aside from possible multiplicative constants. Energy conservation is understood so that $k_a^2 + k_b^2$ is fixed. The important point is that the ionization amplitude $A(\boldsymbol{k}_a, \boldsymbol{k}_b)$ relates directly to the wave function for two electrons in the asymptotic, free particle, limit. Exact zeros appear in momentum distributions; thus the question of their vortex nature immediately arises.

These zeros may be analyzed in the spirit of Ref. [14]; however, it is necessary to discuss the relationship of zeros and vortices in multiparticle wave functions where the dimensions of variable space are greater than three. In n dimensions the requirement that the real and imaginary parts of the generic amplitude $\phi(x_1, x_2, \ldots, x_n) \equiv \phi(\{x\})$ vanish defines a $n - 2$ dimensional hypersurface. It can be shown that integration of the velocity field along a curve in the n-dimensional space enclosing an isolated zero of ϕ equals 2π just as in three dimensions. This point will be elaborated further in a longer, follow-up paper giving details of the analysis presented here.

To analyze the n-dimensional vortices further we note that, at zeros in n dimensions, one can always transform to coordinates such that $\phi(\{x\})$ vanishes linearly in two coordinates x_1, x_2 and quadratically in the remaining $n - 2$ coordinates. For future reference, we call x_1 and x_2 the vortex coordinates. Then the analysis of Ref. [14] carries over almost without change to spaces of arbitrary dimension. In these spaces the velocity field $\boldsymbol{v}(\boldsymbol{x}) = \mathrm{Im}(\phi^* \nabla\phi - \phi\nabla\phi^*)/|\phi|^2 \propto (x_1\hat{\boldsymbol{x}}_2 - x_2\hat{\boldsymbol{x}}_1)/|\phi|^2$ circulates around the zero and is perpendicular to the "radial" vector $\boldsymbol{\rho} = x_1\hat{\boldsymbol{x}}_1 + x_2\hat{\boldsymbol{x}}_2$. Integration of $\boldsymbol{v}(\boldsymbol{x})$ around a path enclosing the zero gives the value of 2π. The zeros of $\phi(x_1, x_2, \ldots, x_n)$ lie on the vortex hypersurface. By fixing the coordinates $x_3, \ldots, x_{j-1}, x_{j+1}, \ldots, x_n$ at the values $x_i = a_i$, $i = 3 \ldots n$, $i \neq j$ of the zero of ϕ, one generates an amplitude $f(x_1, x_2, x_j) = \phi(x_1, x_2, a_3, \ldots, a_{j-1}, x_j, a_{j+1}, \ldots a_n,)$ that has a vortex line in the three-dimensional reduced space x_1, x_2, x_j. The analysis of Ref. [14] can then be directly applied to all of the reduced spaces of three dimensions corresponding to different choices of j.

Murray and Read [11] measured the $(e, 2e)$ cross section in the symmetric geometry and found a deep minimum at an incident energy of 64.6 eV for electrons. In the present case, the momenta $\boldsymbol{k}_a$, $\boldsymbol{k}_b$ with energy conservation define a variable space of five dimensions. For arbitrary $\hat{\boldsymbol{k}}_a$, $\hat{\boldsymbol{k}}_b$ the measured momentum distribution is an incoherent sum of the triplet and singlet amplitudes and an exact zero is unlikely. For the symmetric geometry only the singlet amplitude contributes so that a vortex in the singlet wave function could produce a zero in the momentum distribution. The calculations of Refs. [7,8] reproduce this minimum and locate it near an exact zero. We have repeated the calculations and do indeed find a vortex, described below, near the minimum in the measured TDCS. Since the vortex center must lie at an exact zero, this proves that the minimum is due to a vortex.

To analyze the vortex structure employing Eq. (2) it is essential to work with a pure state described by a wave function, as for the singlet amplitude. The vortex coordinates are the symmetric $\boldsymbol{k}_+ = (\boldsymbol{k}_a + \boldsymbol{k}_b)/2$ and antisymmetric $\boldsymbol{k}_{ab} = (\boldsymbol{k}_a - \boldsymbol{k}_b)/2$ linear combinations of the final state momentum vectors. As is customary for collisions the incident momentum $\boldsymbol{K}_i$ is the z axis and the x axis is in the plane of $\boldsymbol{K}_i$ and $\boldsymbol{k}_+$ with the y axis along $\boldsymbol{K}_i \times \boldsymbol{k}_+$ as in Fig. 1. The symmetric geometry is defined so that the vector $\boldsymbol{k}_{ab}$ is perpendicular to the xz plane and $k_a = k_b$. The amplitude vanishes linearly in the x and z components of $\boldsymbol{k}_+$, quadratically in the y component of k_+, and quadratically in the x and z components of $\boldsymbol{k}_{ab}$, confirming that these are the appropriate vortex coordinates. The y component of $\boldsymbol{k}_{ab}$ is set by energy conservation and is not an independent variable.

The experimental data of Ref. [11] are compared with the DS3C theory of Ref. [7] in Fig. 2, where 2Θ is the angle between the outgoing electron momenta and $\theta_+ = 67.5°$. The computed TDCS agrees qualitatively with the data of

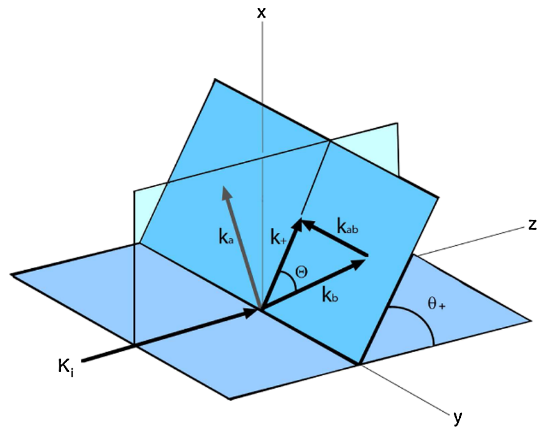

FIG. 1 (color online). (e:2e) coplaner symmetric geometry, showing initial $\boldsymbol{K}_i$ and final $\boldsymbol{k}_a, \boldsymbol{k}_b$ momentum vectors along with $\boldsymbol{k}_+$ and $\boldsymbol{k}_{ab}$ and the angles θ_+, and Θ. The vector $\boldsymbol{k}_{ab}$ is perpendicular to the xz plane and $\boldsymbol{k}_+$ lies in that plane.

Ref. [11], but is sensitive to the approximations employed for the initial helium wave function. It is seen that the present approximation does not give a minimum at exactly the same point as found experimentally. Rather, for $\theta_+ = 67.5°$, the experimental minimum is at $\Theta = 70°$, while the theory has $\Theta = 62.5°$. With more accurate wave functions the position of the minimum shifts but still retains the features identified here [17].

While our calculations find a minimum in the plot shown in Fig. 2, this minimum does not correspond to an exact zero. An exact zero is located on a contour plot of the singlet amplitude in the k_{+x}, k_{+z} plane shown in Fig. 3 for an incident energy of 64.6 eV and the initial and final state wave functions given in Refs. [7,8]. We see that there is an exact zero at $\boldsymbol{k}_+ = (0.522, 0, 0.31)$ corresponding to an angle $\theta_+ = 59.3°$ and a value of $\Theta = 60.0°$. A plot of the computed TDCS that passes through the exact zero is shown in Fig. 2. To show that the exact zero is a vortex, small vectors parallel to the direction of the velocity $\boldsymbol{v}(k_{+x}, k_{+z})$ are shown in Fig. 3. The circulation confirms that the zero in the momentum distribution is, in fact, a vortex. Integration of the velocity field around the zero gives 2π as it must for a single-valued function which vanishes linearly [14]. Conversely, a value of 2π for the integral of the velocity field on a closed path shows that there is a first order zero enclosed by the path. In this way an exact zero is identified without actually hitting it.

The data have a minimum at $\Theta = 70°$. To analyze the depth of the minima Murray and Read [13] deconvolved their data by fitting to a high order polynomial convoluted with an experimental width $\Delta\Theta = w = 8°$. Their fitted curve is shown in Fig. 2(b). The deep minimum indicates that there is a zero and hence a vortex close to $\Theta = 69.6°$ and $\theta_+ = 67.5°$.

In principle, the deconvolved data in Fig. 2 can be used to fit the TDCS to a linear vortex $\boldsymbol{k}_{+v}$ form, i.e.,

$$A(\boldsymbol{k}_+) = \boldsymbol{C} \cdot (\boldsymbol{k}_+ - \boldsymbol{k}_{+v}), \tag{3}$$

where $\boldsymbol{C} = (C_x, 0, C_z)$ is an array of fitting constants C_x and C_z. Since the deconvolution finds the vortex position, we need only fit $\boldsymbol{C}$. We find $C_x = -0.160 + 0.806i$ and $C_z = 0.664 + 0.195i$. The resulting TDCS shown in Fig. 2(b) fits the data near the minimum, but shows some deviation at $\Theta = 80°$ indicating that higher order terms

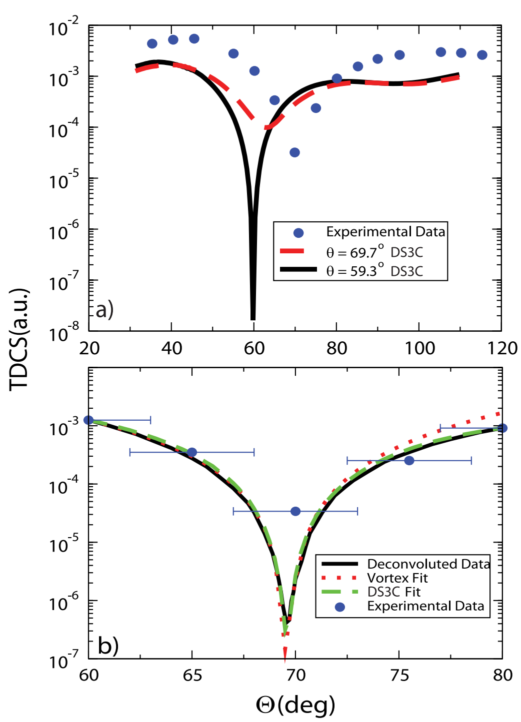

FIG. 2 (color online). (a) The experimental results for $He(e, 2e)He^+$ with $E_a = E_b = 20$ eV and $\theta_+ = 67.5°$ from Ref. [13] (blue dots) compared with the TDCS calculated using the DS3C wave function (red dashed line). Also shown is a theory curve for $\theta_+ = 59.3°$ which goes through the DS3C vortex. (b) Comparison of the deconvolved TDCS of Ref. [13] with a fit to the vortex of Eq. (2). The horizontal lines indicate the width of the convolution function of Ref. [13]. Also shown is a fit obtained by varying parameters in the DS3C amplitude.

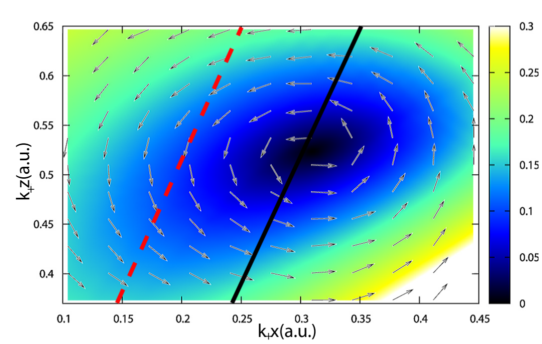

FIG. 3 (color online). Contour plot of $|A(\boldsymbol{k}_a, \boldsymbol{k}_b)|$ on a logarithmic scale. Vectors are drawn in the direction of the current $\boldsymbol{v}$ showing that the minimum in Fig. 2 is near a vortex. The diagonal lines trace the vector $\mathbf{k}_+$ as the angle Θ is varied to produce the DS3C curves in Fig. 2.

are needed. Rather than employ higher order terms we have supposed that the functional form of the DS3C amplitude is correct near the vortex, and have adjusted parameters in that amplitude to fit the vortex position and width. The resulting fit agrees well with the data thus the zero in both experiment and the DS3C cross sections indicate a vortex in the $(e, 2e)$ momentum distribution.

We do not find a vortex in the triplet amplitude, however, since the singlet amplitude is the sum of the direct $A(\boldsymbol{k}_a, \boldsymbol{k}_b)$ and exchange $A(\boldsymbol{k}_b, \boldsymbol{k}_a)$ amplitudes it follows that both the direct and exchange amplitudes have vortices. To analyze the vortex in the direct amplitude, it is useful to employ the momenta $\boldsymbol{k}_a$ and $\boldsymbol{k}_b$ with $\boldsymbol{k}_a$ fixed in the xz plane at the value corresponding to the vortex in Fig. 3. Then the zero is at a value of $\boldsymbol{k}_b$ found by rotating the pair $\boldsymbol{k}_a, \boldsymbol{k}_b$ rigidly about the z axis so that $\boldsymbol{k}_a$ lies in the xz plane. In this frame, the initial state and hence the direct amplitude are invariant to reflections in the plane of $\boldsymbol{K}_i, \boldsymbol{k}_a$ and bound states of electron b have a single component of orientation perpendicular to the xz plane [18]. The vortex shows that the continuum states are also oriented with nonzero components of angular momentum in directions perpendicular to the xz plane.

The connection with orientation shows the relation of vortices to atomic dynamics. Semiclassically, the angular momentum vectors of incident electrons scattered by attractive potentials point parallel to the y axis if incident electrons are scattered upward toward positive x in the coordinate system employed here. The corresponding current circulation is counterclockwise around the y axis. In the collision, the incident electron transfers angular momentum to electron b so that it acquires some angular momentum and therefore also circulates in the counterclockwise sense. If dipole transitions dominate then the vortex position is at $k_{ax} = k_{az} = 0$ and the vortex line is along the y axis. The presence of other multipoles shifts the zero away from this line to places where k_{ax} and k_{az} are nonzero. It is somewhat surprising that the location of the vortex seen in collisions at relatively low impact energies follows this simple prescription.

Previous interpretations of the exact zero have attributed it to interference effects [7,8,10,17]. Reference [17] contrasts the interference of partial waves with the interference between screening and nonscreening terms postulated in Refs. [7,8]. As discussed in Refs. [8,17], the latter effect cannot be present in atomic hydrogen where calculations find a weak minimum. Weak minima that are not isolated zeros can occur where either ReA or ImA vanish, whereas both terms must vanish at the same point for vortices. Our calculations for H (not shown) find no vortices indicating that the minima seen in DS3C calculations [8] for H differ from those in He.

The calculations of Ref. [17] fit the experimental data very accurately at $\theta_+ = 67.5°$ and $E = 64.6$ eV up to a normalization constant. We have used the parametrized DS3C to fit the minima at 67.5° found in Ref. [17] for $E =$ 64.6 eV, and then evaluated the vortex position for that fit. We find a vortex at $\theta_+ = 62.1°$ and $\Theta = 70°$ in good agreement with the position of the deepest minima found in Ref. [17].

In retrospect one can recognize exact zeros in earlier calculations for other systems. For example, exact zeros are seen in Coulomb Born calculations of inner shell ionization [19]. In that case, a partial wave analysis shows vortices due to continuum-state orientation.

In summary, the present results complement the list of structures in $(e, 2e)$ TDCS given in Ref. [9]. They also realize the insight given in Ref. [14] that vortices in atomic wave functions must have observational consequences. Such consequences have been predicted theoretically and are now verified for actual observations.

This research is sponsored by the Office of Basic Energy Sciences, U.S. Department of Energy under Grant No. DE-FG02-02ER15283. Travel support for one of us (J. H. M.) by the Max-Planck Institute for Complex Systems is gratefully acknowledged. J. S. B. acknowledges support from the DFG under Contract No. Br728/13-1.

*Permanent address: Ioffe Physical Technical Institute, St. Petersburg, Russia.

[1] E. Weigold and I. E. McCarthy, *Electron Momentum Spectroscopy* (Kluwer Academic, New York, 1999).
[2] T. N. Rescigno, M. Baertschy, W. A. Isaacs, and C. W. McCurdy, Science **286**, 2474 (1999).
[3] I. Bray, K. Bartschat, and A. T. Stelbovics, Phys. Rev. A **67**, 060704 (2003).
[4] J. Colgan and M. S. Pindzola, Phys. Rev. A **74**, 012713 (2006).
[5] A. T. Stelbovics, I. Bray, D. V. Fursa, and K. Bartschat, Phys. Rev. A **71**, 052716 (2005).
[6] J. Colgan, M. S. Pindzola, G. Childers, and M. Khakoo, Phys. Rev. A **73**, 042710 (2006).
[7] J. Barakdar and J. S. Briggs, Phys. Rev. Lett. **72**, 3799 (1994).
[8] J. Berakdar and J. S. Briggs, J. Phys. B **27**, 4271 (1994).
[9] J. S. Briggs, Comments At. Mol. Phys. **23**, 155 (1989).
[10] M. S. Pindzola (private communication).
[11] A. J. Murray and F. H. Read, J. Phys. B **26**, L359 (1993).
[12] O. Al-Hagan, C. Kaiser, D. H. Madison, and A. J. Murray, Nature Phys. **5**, 59 (2009).
[13] A. J. Murray and F. H. Read, Phys. Rev. A **47**, 3724 (1993).
[14] I. Bialynicki-Birula, Z. Bialynicka-Birula, and C. Sliwa, Phys. Rev. A **61**, 032110 (2000).
[15] J. H. Macek, J. S. Sternberg, S. Y. Ovchinnikov, T-G. Lee, and D. R. Schultz, Phys. Rev. Lett. **102**, 143201 (2009).
[16] J. H. Macek and S. Y. Ovchinnikov, Phys. Rev. Lett. **80**, 2298 (1998).
[17] J. Colgan, O. Al-Hagan, D. H. Madison, A. J. Murray, and M. S. Pindzola, J. Phys. B **42**, 171001 (2009).
[18] U. Fano and J. H. Macek, Rev. Mod. Phys. **45**, 553 (1973).
[19] J. Botero and J. H. Macek, Phys. Rev. A **45**, 154 (1992).